Development and calibration of the LASER Pattern Shift Method for measuring the lamella topology during drop impact on walls

Patrick Foltyn*[1], Norbert Roth[1], Bernhard Weigand[1]
[1]University of Stuttgart, Institute for Aerospace Thermodynamics (ITLR), Pfaffenwaldring 31, 70569 Stuttgart, Germany
*Corresponding author: patrick.foltyn@itlr.uni-stuttgart.de

Abstract
Spreading behavior of droplets impinging on flat walls have been and still are often investigated. However, the experimental investigation of the lamella thickness and shape is very difficult due to the outer rim hiding the inside. For these investigations a new measurement method was developed measuring the lamella height profile along one axis. Additionally, this method can be used for time-resolved monitoring of lubricating films and component spacing in the range of a few micrometers up to several millimeters.
This paper validates the proposed technique presenting the derivation of the describing equation and the experimental setup. For validating the thickness measurement of the lamella during a droplet impact, the time dependent film thickness of an evaporating isopropanol film with an initial thickness of approximately $300\mu m$ is measured. The results of the newly proposed method using a LASER line as pattern are compared to a commercial system based on confocal chromatographic interference (CCI) and an analytical solution for the mass transfer.

Keywords
droplet impact, lamella topography, thickness measurement, total internal reflection, film evaporation

Introduction

For layer thickness measurements, especially for liquid films, there are many different methods, which are described e.g. in Tibiriçá et al. (2010), [1]. The methods can be classified, based on their operating principle, into acoustical, electrical, optical, and nucleonic techniques. This paper proposes a new optical method for film thickness measurements.
Among many different optical approaches for measuring the film thickness, techniques based on total internal reflection and confocal chromatic interference are commonly employed.
Experiments using total internal reflection of the interface for measuring thin liquid films between a maximum of a few hundred micrometer up to a few millimeter were conducted by Than et al. [2] and Yu et al. [3]. Very low film thicknesses down to 1 nm were measured by Heavens and Gingell [4] using frustrated total reflection fluorescence.
The confocal chromatic interference approach is also used in commercial systems of microEpsilon [5] or Precitec [6]. Lel et al. [7] and Jakob [8] described in detail the principle of CCI measurements. In short, the principle is based on reflection of polychromatic light at interfaces. Due to the chromatic aberration of lenses the focal point for reflected light of each color is in a different plane. With the help of the confocal optical setup mainly the light color having its focal spot in the aperture is let through and analyzed by a spectrometer. A calibration curve enables the calculation of the film thickness as a function of the light color analyzed by the spectrometer.
However, the intensity of reflected light, calculated by Fresnel's equations, is dependent on the difference between the refractive indices of the adjacent layers. Often, these differences are not high enough to be able to measure very thin films or detecting interfaces since some intensities of the reflected light are too low. This could be also seen in the experiments of this paper where intensities of the liquid-glass interface were almost as low as the noise level. Also Let et al. [7] have reported problems in thickness determination for low intensities. Additionally, the wavelength dependent refractive index $n(\lambda)$ of the used materials needs to be known because of the polychromatic light source.
For measuring the lamella thickness during the droplet impingement non of the above-mentioned methods is suitable for several reasons: Firstly, many methods have a limited measurement range, especially at small film thicknesses. Most commercial systems provide therefore many different and often costly sensors, each for a limited measurement range. Since the lamella thickness will vary very fast over a wide range, several sensors need to be used concurrently. Secondly, the sensor axis must be aligned to the droplet impact axis leading to interference with the droplet fall trajectory. And further, a measurement from the bottom of the glass wall might not be feasible due to low intensity of reflected light, small working distance, etc. Thirdly, systems which are using reflected light from each interface will have a very low intensity in reflected light. Fourthly, many systems usually offer only small measurement spots, which are ideal only for point-measurements. Thickness measurements along one line or for a whole area need to be achieved by scanning the lamella topography. This is not feasible due to the short time scale of droplet impact dynamics. For these reasons, a new experimental method, capable of rapid measurements of film/lamella thickness along a line for droplet impact on wall, is developed.
The new LASER pattern shift method (LPSM) uses the total internal reflection in liquid films or transparent layers. Hereby, it was found that the displacement of a pattern projected by a LASER onto the surface is proportional to the film height. As a consequence, a very accurate measurement setup can be build, comparable to available

commercial systems for film thickness measurements. However, the new setup is significantly more flexible in the measuring range allowing a measurement of highly variable film thickness over several orders of magnitude.
In what follows, the details of LPSM are discussed. LPSM is then applied for validation to measure the temporal variation of the thickness of a flat, evaporating wall-film. Further, these film thickness measurements are compared to the corresponding CCI-based measurements as well as an approximate analytical solution for the thickness of an evaporating thin film.

Experimental setup and detailed discussion of the new LPSM measurement method

Experimental setup

The experimental setup consists of two separate apparatus to measure the film thickness: the newly proposed LASER Pattern Shift Method (LPSM) and an often-used and reliable method based on Confocal Chromatic Interference (CCI). The CCI apparatus (micro-Epsilon IFC2451), which is able to measure a minimal film thickness of approximately $140\mu m$, and the LPSM apparatus are used to measure the film thickness at the same spot of the test film in order to control the measurements (see Figure 1). The newly proposed device consists of three main modules: a LASER pattern generating module (#1), a prism on which a liquid film is placed (#2) and a camera with an optical lens (#3). For the reported results, a LASER line was used as pattern. On the horizontal plane of the prism a circular ring with a diameter of $32mm$ and a height of $1.5mm$ is glued forming a liquid reservoir. This reservoir is filled at the beginning of each measurement with isopropanol (2-propanol) using a calibrated pipette (BRAND Transferpette® S $100 - 1000\mu L$) in order to know exactly the volume of liquid inside the pool. The position of the LASER line is detected by a monochromatic camera (IDS uEye UI-3080SE-M-GL) which is mounted to a Zoom Lens System (Navitar 12x Zoom lens MVL12X3Z in combination with 2x lens MVL12X20L).
The decreasing film thickness of the evaporating isopropanol film, with an initial height of approximately $300\mu m$, was measured in the middle of the pool at a frequency of $1Hz$. This is sufficiently fast since the decreasing velocity of the film thickness was quite low. The post-processing to determine the film thickness was done using a computer for both measuring techniques.
The description of the working principle and the derivation of the correlation (Eq. (14)) between the LASER pattern shift and the film thickness are given in the following section.

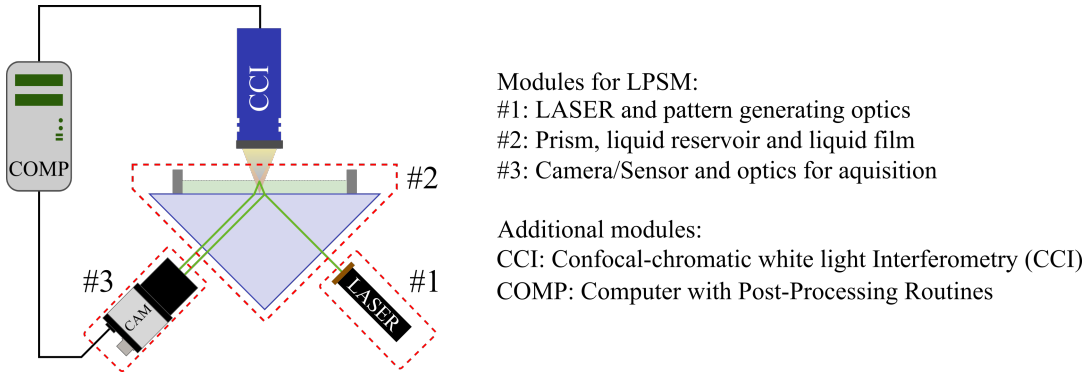

Figure 1. Experimental setup with the LPSM and the CCI modules for film thickness measurements

Measurement principle of LPSM

Before an analytical correlation is derived, the basic principle of the measurement setup is explained using a simple configuration which was also used for the validating film thickness measurements (see Figure 2). It can be seen as an extraction of module #2 of Figure 1. In the following, a single beam shall represent an arbitrary LASER pattern.
The measurement technique LPSM based on the LASER pattern shift uses the total internal reflection on interfaces. At first, a reference measurement needs to be performed initializing the system to the "dry state", see ray 1 in Figure 2 a). Afterward, a liquid film is created on the prism leading to a shift of the LASER pattern by a distance d_{CAM} on the camera, see ray 2 in Figure 2 b). Although, the intensity of ray 1 can be calculated by Fresnel's equations, it is not detectable by the camera. As a consequence, ray 1 will be neglected during a wetted case in the following. Additionally, it is a demonstration of the significant advantage of this method compared to existing methods based on reflection. The light intensity of the transmitted beam is always sufficiently high, while the reflected beam, e.g. in CCI, depends on the ratio of the refractive indices of the interface. If this ratio is too small no usable signal can be detected.

Analytical derivation for LPSM

For the analytical derivation of the correlation between the LASER pattern shift d_{CAM} on the camera sensor and the film thickness h_F, a more complicated case shall be used, see Figure 3. With this case, it can be shown that only the added film height to the reference measurement has an influence on d_{CAM}. This represents the general case and might be important if, e.g., a special surface or glass plate is placed on the prism on which then the droplet impingement occurs. In order to get the LASER pattern to the upper surface on which the measurement should take place, a coupling medium must be used.

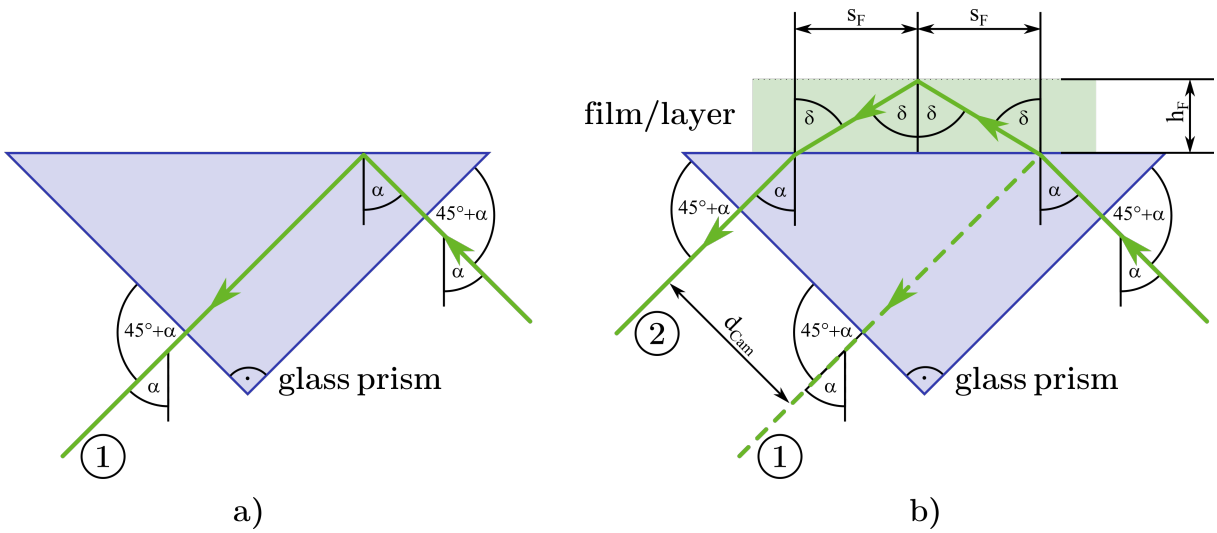

Figure 2. Ray tracing of LASER beams in experimental setup; a): Ray trajectory with dry surface (reference case), b): Ray trajectory with applied liquid film

For the analytical derivation, the laws of reflection derived from the Fresnel's equations, trigonometrical relations and Snell's Law (1), are necessary. The refraction at an interface, resulting in an exiting angle ξ_2 is herein dependent from the refractive indices of both adjacent media and the inclination angle ξ_1

$$n_1 \sin \xi_1 = n_2 \sin \xi_2 \tag{1}$$

Starting with the incident ray on the right side of Figure 3, the ray hits the right lower surface of the prism with an angle of $45° + \alpha$ which is for the present case with $\alpha = 45°$ equal to $90°$. On the upper prism surface, the LASER line is refracted with an angle of β into the coupling medium. Again, this ray is refracted at the interface between coupling medium and the intermediate plate with an angle γ. On the upper surface of the intermediate plate, there will be a total reflection in case of a dry surface, analogous to Figure 2 a). The ray will pass all interfaces again with the corresponding diffraction angles γ, β and α and will finally exit the prism shown as ray 1 in Figure 3. In case of a liquid film on top of the intermediate plate the incident ray is refracted one additional time with an angle δ. After the total reflection on the upper gas-liquid interface, the LASER pattern will exit the prism taking the path of ray 2 in Figure 3. The angles can all be calculated by applying Snell's Law (equation (1)) several times resulting in the following equations:

$$n_P \sin \alpha = n_C \sin \beta \tag{2}$$
$$n_C \sin \beta = n_G \sin \gamma \tag{3}$$
$$n_G \sin \gamma = n_F \sin \delta \tag{4}$$

The magnitude of refraction is only depending on the ratio of the refractive indices n_i/n_j of the adjacent layers. Using equations (2) to (4) gives the following relation

$$n_P \sin \alpha = n_G \sin \gamma = n_F \sin \delta \ , \tag{5}$$

verifying that there is only a parallel shift of rays by crossing an arbitrary number of interfaces.
The horizontal shift s_i of the LASER pattern in each layer is according to equation (6) depending on the film height h_i and the angle ξ relative to the surface normal at the interface where the incident ray falls.

$$\frac{s_i}{h_i} = \tan \xi \tag{6}$$

Each horizontal shift can be then calculated as follows

$$s_C = h_C \tan \beta \tag{7}$$
$$s_G = h_G \tan \gamma \tag{8}$$
$$s_F = h_F \tan \delta \tag{9}$$

Using equations (7) to (9), the total horizontal shift s_{tot} caused by a film thickness h_F can be geometrically calculated from Figure 3 as follows

$$s_{tot} = 2\left(s_C + s_G + S_F\right) - 2\left(s_C + s_G\right) = 2s_F \tag{10}$$

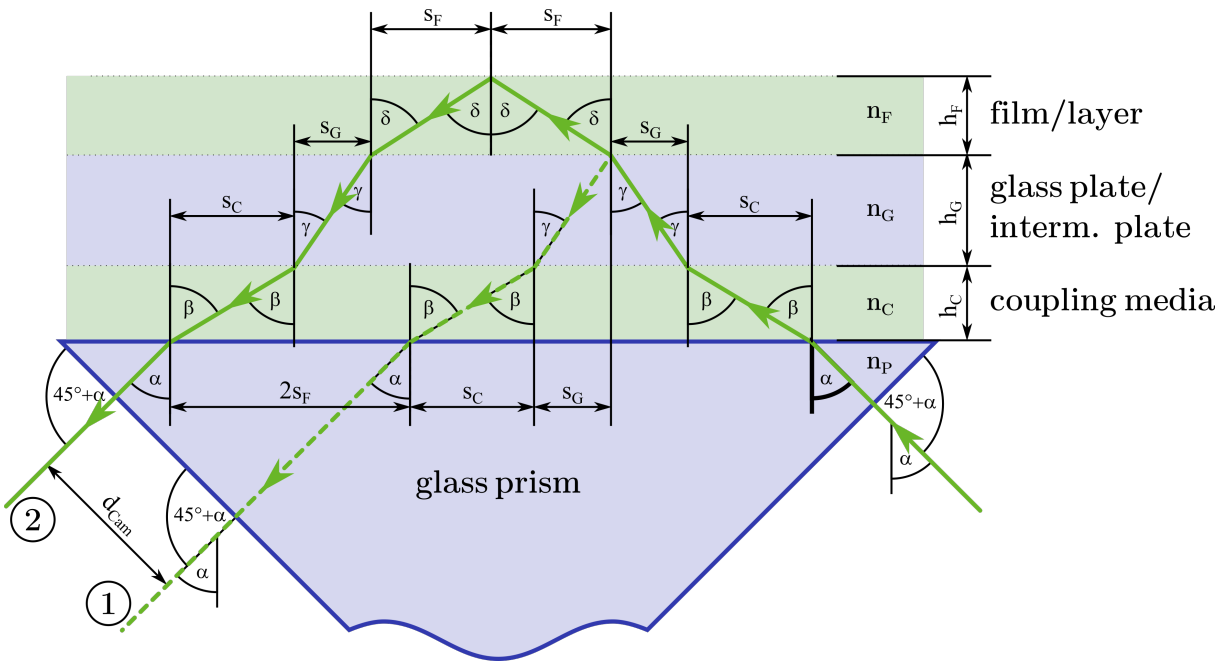

Figure 3. Ray tracing of LASER beams in experimental setup with additional coupling media and intermediate plate

Equation (10) shows impressively that only the added film height causes a pattern shift. Inserting equation (5) into equation (9) leads to

$$s_F = h_F \tan\left(\arcsin\left(\frac{n_P}{n_F}\sin\alpha\right)\right) \tag{11}$$

With the help of the trigonometrical relation $\tan(\arcsin(x)) = \frac{x}{\sqrt{1-x^2}}$ equation (11) can be simplified to

$$s_F = h_F \frac{\frac{n_P}{n_F}\sin\alpha}{\sqrt{1-\left(\frac{n_P}{n_F}\right)^2\sin^2\alpha}} \tag{12}$$

The total horizontal shift s_{tot} can be related to the shift of the LASER pattern on the camera d_{CAM} by the following geometrical consideration

$$s_{tot} = \frac{d_{CAM}}{\cos\alpha} \tag{13}$$

Finally, equations (10),(12) and (13) can be combined to describe the film height h_F as a function of d_{CAM}, n_F, n_P and α

$$h_F = \frac{1}{2} d_{CAM} \frac{n_F}{n_P} \frac{1}{\sin\alpha\cos\alpha} \sqrt{1-\left(\frac{n_P}{n_F}\right)^2\sin^2\alpha} \tag{14}$$

If the scale factor for d_{CAM} is determined by a calibration, the film height can be easily calculated. If no calibration is available, the film thickness h_F can be calculated only relative to the pixel size of the camera.

Experimental procedure and analytical modeling

Experimental procedure

In this section, the experimental procedure is described. Firstly, the reference measurement was done for the LPSM. Secondly, the reservoir was filled with isopropanol using the calibrated pipette and the measurement was started. After the isopropanol was fully evaporated the data was saved on the computer and the post-processing routine was started.

For the CCI, no real post-processing was needed, since the system performed all measurements in real-time using the refractive index $n(\lambda)$ predefined by the user.

The post-processing of the LPSM was, in comparison to the CCI, more complex since the shifted distance d_{CAM} on the camera sensor had to be determined. Exemplarily, Figure 4 shows the raw images from the camera for the dry case (Figure 4 a)) and the wetted case with a film height of $305\mu m$, see Figure 4 b). The resolution of the camera in the direction of d_{CAM} was set to $0.78\mu m/px$ and consequently to $0.46\mu m/px$ in the direction of h_F. The observed shift on the camera was $d_{CAM} = 672px$.

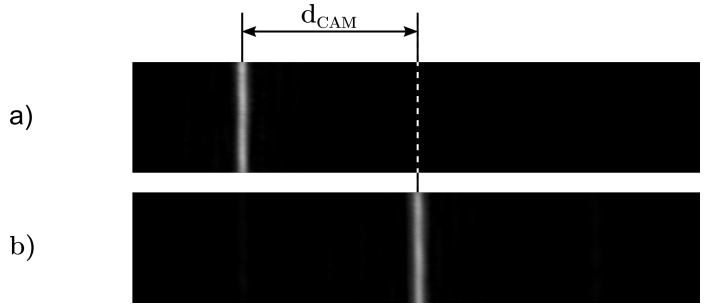

Figure 4. Comparison of the raw images of the monochromatic camera with a) a dry wall and b) a film height of about $305\mu m$. The shift of the LASER line corresponds to $d_{CAM} = 672px$ at an image resolution of $0.78\mu m/px$

To determine d_{CAM}, noise of the image was removed by isolating the LASER line in each image and subtracting areas from the input image which have an intensity lower then a predefined threshold. Then, a cross-correlation gives the shift of each image of the wetted case with respect to the dry reference case, Figure 4 a). With the previously derived correlation (14) the film height h_F can be then computed.
Due to the evaporating film a continuous decrease in film thickness has to be expected which was measured with both techniques, LPSM and CCI, see Figure 5.

Material properties
During the experiments the ambient temperature was measured to be $T = 293K$ and a total pressure of $p_\infty = 1bar$ was assumed. For the vapor phase the ideal gas equation was used in calculating the density of ambient air $\rho_\infty = 1.188kg/m^3$ and the density of the isopropanol-air mixture in the boundary layer $\rho_{BL,mix} = 1.243kg/m^3$. The partial density of isopropanol vapor in the boundary layer is $\rho_{BL,vap} = 0.1060\ kg/m^3$. The ambient air is assumed to be free of isopropanol. The viscosity of dry air, which was assumed by a mixture of 80% Nitrogen and 20% Oxygen, was calculated to $\nu_{air} = 15.31 \cdot 10^{-6} m^2/s$, [9]. The properties of isopropanol are listed in Table 1. The binary diffusion coefficient D of isopropanol was experimentally determined by [10] at $299K$ ambient air temperature. In order to get a diffusion coefficient at $293K$ the proportionality of the diffusion coefficient $D \propto T^{3/2}$ was used, [10]. The refractive index of isopropanol (2-propanol) was taken from Kozma et al. (2005), [11], who have performed their experiments at $295K$. The small temperature deviation between the present experiments and the experiments of [11] was neglected owing to the low temperature sensitivity of the refractive index of liquids. The empirical Cauchy dispersion formula, presented in [11], was used to finally calculate the refractive index of isopropanol at the used LASER wavelength of $533nm$.

Table 1. Properties of isopropanol (2-propanol)

	value	unit	reference
density ρ_{fl}	785	$[kg/m^3]$	[12]
dyn. viscosity μ_{fl}	2.43	$[mPas]$	[12]
saturation pressure p_{sat}	4300	$[Pa]$	[12]
diffusion coefficient D @ $299K$	$9.9 \cdot 10^{-6}$	$[m^2/s]$	[10]
refractive index n_{fl} @ 533 nm	1.3793	$[-]$	[11]

Approximate analytical derivation of the thickness of an evaporating liquid film
In this section, an analytical solution shall be derived describing the idealized mass transfer of an evaporating liquid film. Later, the experimental results will be then compared to the analytical solution.
At first, the Grashof number Gr, Schmidt number Sc, Rayleigh number Ra and Sherwood number Sh are defined by equations (15) to (18) [13]. The inner diameter of the reservoir of $32mm$ was used as characteristic length L_{ch}.

$$Gr = g \frac{|\rho_{BL,mix} - \rho_\infty|}{\rho_\infty} \frac{L_{ch}^3}{\nu_{air}^2} \tag{15}$$

$$Sc = \frac{\nu_{air}}{D} \tag{16}$$

$$Ra = GrSc \tag{17}$$

$$Sh = \frac{k_c L_{ch}}{D} \tag{18}$$

Using the analogy of heat and mass transfer the Sherwood number Sh can be calculated by $Sh = C\ Ra^n$ depending on the Rayleigh number and on the coefficients C and exponent n dependent on the flow regime [13]. Combining equations (15) to (18) gives

$$\frac{k_c L_{ch}}{D} = C \left[\frac{g}{D} \frac{|\rho_{BL,mix} - \rho_\infty|}{\rho_\infty} \frac{L_{ch}^3}{\nu_{air}} \right]^n \tag{19}$$

The mass transfer coefficient k_c in equation (18) is dependent on the molar transfer rate and the concentration gradient of vapor between the boundary layer and the ambient air, see equation (20). k_c can be transformed to equation (21) so that it is dependent on the liquid mass flux $\dot{m}_{fl,A}$ and the difference in the partial density of the transferred species between the boundary layer $\rho_{BL,vap}$ and the ambiant air $\rho_{\infty,vap}$.

$$k_c = \frac{\dot{n}_A}{A\Delta c_A} \tag{20}$$

$$k_c = \frac{\dot{m}_{fl,A}}{(\rho_{BL,vap} - \rho_{\infty,vap})} \tag{21}$$

The partial density of isopropanol vapor in ambient air can be assumed to be $\rho_{\infty,vap} \approx 0$. The decreasing film thickness with time $\dot{h}$ can be calculated with the liquid mass flux and is equivalent to the velocity of the liquid front of the liquid-vapor interface.

$$\dot{h} = \frac{\dot{m}_{fl,A}}{\rho_{fl}} \tag{22}$$

Including equations (21) and (22) into equation (19) gives finally a relation for the decreasing film front velocity $\dot{h}$.

$$\dot{h} = C \left[\frac{g}{D} \frac{|\rho_{BL,mix} - \rho_\infty|}{\rho_\infty} \frac{L_{ch}^3}{\nu_{air}} \right]^n \frac{D}{L_{ch}} \frac{\rho_{BL,vap}}{\rho_{fl}} \tag{23}$$

With the help of the properties of the isopropanol-air mixture and the values of Table 1 one obtains $Sc = 1.594$, $Gr = 6.338 \cdot 10^4$ and $Ra = 1.010 \cdot 10^5$. According to Incropera et al. [13], $C = 0.54$ and $n = 0.25$ need to be defined for laminar flow so that the film front velocity $\dot{h}$ for a laminar free flow regime results in

$$\dot{h} = 0.54 \cdot g^{\frac{1}{4}} D^{\frac{3}{4}} L_{ch}^{-\frac{1}{4}} \rho_\infty^{-\frac{1}{4}} \nu_{air}^{-\frac{1}{4}} \frac{\rho_{BL,vap}}{\rho_{fl}} \left(|\rho_{BL,mix} - \rho_\infty|\right)^{\frac{1}{4}} \tag{24}$$

The analytical film front velocity $\dot{h}$ for the laminar flow can be then calculated to approximately $\dot{h} = 3.905 \cdot 10^{-7} m/s$.

Results and discussion

According the "Experimental procedure"-section, several measurements have been performed. Figure 5 shows the result for 400 seconds of one exemplary measurement. A measurement time of maximum 400 seconds was chosen to make sure that the CCI is still not too close to its lower measurement limit of approximately $140 \mu m$. As expected, the film height h_F is constantly decreasing and both measurement techniques show very similar results, see Figure 5 a). The relative deviation of the measurement values between both techniques are mostly below 4%, see Figure 5 b).

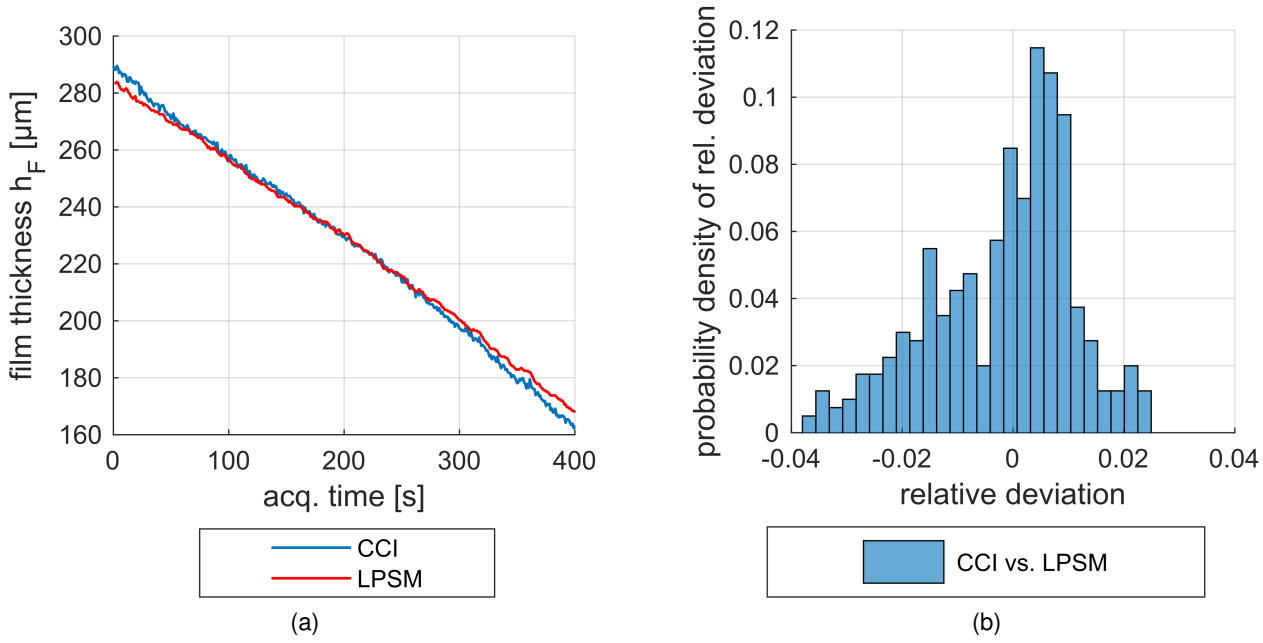

Figure 5. Film thickness measurement over 400 seconds; a): Time dependent measured film thickness with LPSM and CCI, b): Relative deviation between the measurements of LPSM and CCI

The shown behaviors could be reproduced very well by all other measurements as well. Consequently, the decreasing film height was fitted by a straight line with a linear least square approach and a bi-square weighting. The

coefficient of determination, R^2, was always larger than 0.995. The slope of each fitted line was used as experimental film front velocity $\dot{h}$. All velocities were in a range between $0.339\mu m/s$ and $0.284\mu m/s$ and are, therefore, in the expected magnitude as predicted by the analytical solution. The fitted experimental measurements are compared to the analytical solution in Figure 6. The maximal error of the analytical solution in equation (24) was estimated by a linear error propagation. The binary diffusion coefficient D and the saturation pressure p_{sat} contribute most to the error due to a lack of literature date, their high sensitivity to temperature, and the exponential dependence of film front velocity on these parameters. Additionally, no detailed influence of the experimental test rig, e.g. parts and accessories, influencing the free flow and thus the mass transfer have been considered. This influence, as well as other deviations from an ideal analytical case, can be reasons for the deviation between the measurements and the analytical solution. However, the analytical prediction can give an estimate of the magnitude and justifies a proper experimental procedure.

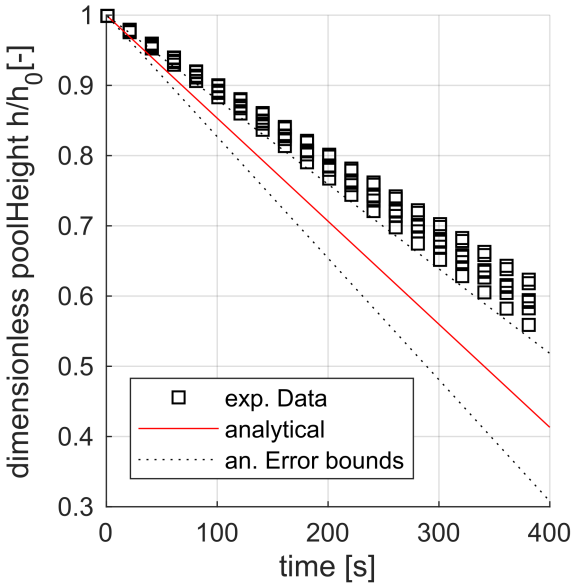

Figure 6. Fitted dimensionless film thickness over 400 seconds measured with LPSM and compared with analytical model.

Although the measurements values of both measurement systems, LPSM and the CCI, are not strongly deviating, there can be potential factors causing a deviation and these should be identified. Slight temperature fluctuations might induce internal currents in the liquid film leading to a wavy surface caused by Marangoni currents as reported by Lel et al. (2008) [7]. A parallel pair of surfaces (glass surface and film surface) is very crucial for both methods. In general, the refractive index is the basis of measurement for both techniques. Therefore, the wavelength dependent refractive index $n(\lambda)$ of the substances must be known very well for the CCI. A changing film height leads to a different color interference in the aperture, see the "Introduction"-section. If the wavelength dependent refractive index $n(\lambda)$ is not properly defined slight deviations between measured and real film height can occur. For the LPSM this knowledge is only necessary for the LASER wavelength. A misalignment of the measurement spot, respectively line, of both systems can be neglected, because they were aligned to each other with a deviation smaller than a few hundred micrometers. This is considered to be sufficiently accurate because the film height will not change dramatically over this length scale.
As a result, it could be shown that both measurement methods delivered consistent measurement values. The measurement range of the CCI was deliberately not exceeded so that a reliable evaluation of the measurement results can be made. However, since it is to be expected that the drop lamella is significantly thinner than $140\mu m$, thinner films will have to be measured in future. For theses smaller thicknesses the LPSM shows strong advantages and guarantees reliable results!

Conclusions

In the present paper, a potential new measurement method (LPSM) for measuring the lamella thickness field during a droplet impact was presented. Its principle is based on the shift of a LASER pattern. Measurements of a decreasing isopropanol film with an initial height of approximately $300\mu m$ were performed with the new method and compared to a commercial system based on Confocal Chromatic Interferometry (CCI) in order to show the capability of the new method. Additionally, an approximate analytical solution for the decreasing film height velocity was derived. The results agree very well between both measurement techniques and also with the analytical solution. Deviations can be explained by influences which were not taken into account during the idealized approximate analytical estimation.
The capability of LPSM to measure film thicknesses of order of $100\mu m$ is demonstrated in the current study. This also holds a strong promise for measuring lower film thicknesses where CCI is not capable. This is being explored

in the ongoing investigations.

Acknowledgments
The authors kindly acknowledge Prof. Yuri Zudin and Dr. Visakh Vaikuntanathan for the very fruitful discussions. In addition, the authors kindly acknowledge the financial support of this work by the Deutsche Forschungsgemeinschaft (DFG) in the frame of the International Research Training Group "Droplet Interaction Technologies" (GRK 2160/1: DROPIT)

Nomenclature

Latin symbols:

d_{CAM}	shift of LASER pattern on camera sensor
D	binary diffusion coefficient [m^2/s]
g	gravitational acceleration (=9.81 m/s)
h	height
$\dot{h}$	film front velocity [m/s]
k_c	mass transfer coefficient [m/s]
$\dot{m_{fl,A}}$	mass flux [kg/(m^2 s)]
n_i	refractive index
Gr	Grashof number [-]
L_{ch}	characteristic length [m]
Ra	Rayleigh number [-]
s	horizontal shift
Sc	Schmidt number [-]
Sh	Sherwood number [-]

Greek symbols:

$\alpha, \beta, \gamma, \delta, \xi$	angles [°]
ν	kinematic viscosity [m^2/s]
ρ	density [kg/^{3}]
λ	wave length [nm]

subscripts:

air	dry air
BL	boundary layer
C	coupling media
F	film
fl	fluid
G	intermediate glass plate
mix	vapor-air mixture
P	prism
tot	total
vap	vapor
∞	in (infinite) ambiance

References

[1] Tibiriçá, C. B., do Nascimento, F. J., and Ribatski, G., 2010. "Film thickness measurement techniques applied to micro-scale two-phase flow systems". *Experimental Thermal and Fluid Science,* ***34***(4), pp. 463 – 473.

[2] Than, C. F., Tee, K. C., Low, K. S., and Tso, C. P., 1993. "Optical measurement of slope, thickness and velocity in liquid film flow". *Smart Materials and Structures,* ***2***(1), pp. 13–21.

[3] Yu, S., Tso, C., and Liew, R., 1996. "Analysis of thin film thickness determination in two-phase flow using a multifiber optical sensor". *Applied Mathematical Modelling,* ***20***(7), pp. 540 – 548.

[4] Heavens, O., and Gingell, D., 1991. "Film thickness measurement by frustrated total reflection fluorescence". *Optics & Laser Technology,* ***23***(3), pp. 175 – 179.

[5] Micro-Epsilon. confocaldt // confocal chromatic measuring system. `https://www.micro-epsilon.com/download/products/cat--confocalDT--en.pdf`.

[6] PRECITEC OPTRONIK, 2018. Optical sensors. `https://www.precitec.de/fileadmin/uploads/overview/sensors_EN.pdf`.

[7] Lel, V. V., Kellermann, A., Dietze, G., Kneer, R., and Pavlenko, A. N., 2008. "Investigations of the marangoni effect on the regular structures in heated wavy liquid films". *Experiments in Fluids,* ***44***(2), pp. 341–354.

[8] Jakob, G., 2000. "Koaxiale interferometrische schichtdickenmessung". *Sonderdruck aus Photonik,* ***3***.

[9] Lemmon, E. W., and Jacobsen, R. T., 2004. "Viscosity and thermal conductivity equations for nitrogen, oxygen, argon, and air". *International Journal of Thermophysics,* ***25***(1), pp. 21–69.

[10] Gilliland, E. R., 1934. "Diffusion coefficients in gaseous systems". *Ind. Eng. Chem.,* ***26***(6), pp. 681–685.

[11] Kozma, I. Z., Krok, P., and Riedle, E., 2005. "Direct measurement of the group-velocity mismatch and derivation of the refractive-index dispersion for a variety of solvents in the ultraviolet". *J. Opt. Soc. Am. B,* ***22***(7), pp. 1479–1485.

[12] Th.Geyer, 2017. Safety data sheet according to 1907/2006/ec, article 31. Tech. rep., Th. Geyer GmbH & Co. KG.

[13] Incropera, F. P., Dewitt, D. P., Bergman, T. L., and Lavine, A. S., 2007. *Fundamentals of Heat and Mass Transfer*, Vol. 6. John Wiley & Sons Inc.